

# Nuclear fragmentation cross section measurements with the FOOT experiment

Riccardo Ridolfi<sup>1,2,\*</sup>

<sup>1</sup>INFN, Sezione di Bologna - Bologna, Italy

<sup>2</sup>Dipartimento di Fisica e Astronomia "Augusto Righi", Università di Bologna - Bologna, Italy

**Abstract.** Different fields can profit by nuclear fragmentation cross section measurements: among them hadrontherapy and space radioprotection are of particular interest. Hadrontherapy employs high-energy beams of charged particles (protons and heavier ions) to treat deep-seated tumours. In these treatments nuclear interactions have to be considered: beam particles can fragment in the human body releasing a non-zero dose beyond the tumour while fragments of human body nuclei can modify the dose released in healthy tissues. On the radioprotection side, the interest in long-term manned space missions beyond Low Earth Orbit is growing in these years but it has to cope with significant health concerns from radiation in space, necessitating an accurate cross section data description. The FOOT (FragmentatiOn Of Target) experiment was proposed to cover these gaps in data. It was designed to detect, track and identify nuclear fragments and aims to measure double differential cross sections both in angle and kinetic energy which is the most complete information to address existing questions. The FOOT experimental setups, the experimental program and a first cross section analysis of 400 MeV/u <sup>16</sup>O beam on Carbon target data acquired in July 2021 at GSI (Darmstadt, Germany) will be presented.

## 1 Introduction

Hadrontherapy is an external radiation therapy technique in which protons and heavier ions are used to treat deep-seated solid tumours. The main advantage to use charged particles to treat tumours is their favourable depth-dose profile which is very different from that of photons used in conventional radiation therapy. Indeed, while a photon beam reduces its intensity exponentially as it enters into a material, charged particles are characterised by a low energy release in the beginning followed by a sharp rise after which the particle stops (Bragg peak). This behaviour makes charged particles particularly suitable to treat tumours near critical organs that must be spared by the radiation, especially in younger patients. Moreover, the electric charge of hadrons allows to actively move the beam to cover all the tumour volume. Furthermore, heavier ions such as Carbon and Oxygen can play an important role in treating radioresistant tumours thanks to their enhanced biological effectiveness. However, nuclear interactions have to be accounted for: beam particles can fragment in the human body producing lower mass nuclei able to release a non-zero dose beyond the Bragg peak. This contribution has to be properly described. On the other hand, nuclear interactions providing the fragmentation of nuclei of the human body give rise to fragments with low energy. These nuclear fragments can modify the dose released in healthy tissues and their effects are still in question given the lack of accurate cross sections data. The study of such nuclear

interactions is of strong interest also in the space radioprotection field. Indeed, the interest in long-term manned space missions beyond the Low Earth Orbit is growing in these years. However, the health risks linked to space radiation are a major hazard which can potentially prevent any mission due to unacceptable risks for the astronauts since huge gaps in fragmentation cross sections data used to benchmark both deterministic and Monte Carlo models are present. Among all the possible measurements, double differential cross sections, both in angle and kinetic energy, would be the most significant contribution of experimental nuclear physics to these fields providing the most complete information to develop a new generation of treatment planning systems for patients and reliable transport codes and risk models for space radioprotection.

## 2 The FOOT experiment

To address all these questions, the FOOT (FragmentatiOn Of Target) experiment was proposed. It is composed by two independent and complementary setups, an Emulsion Cloud Chamber and an electronic setup composed by several subdetectors providing redundant measurements of kinematic properties of fragments produced in nuclear interactions between a beam and a target. FOOT was designed to detect, track and identify nuclear fragments and aims to measure double differential cross section both in angle and kinetic energy relevant for hadrontherapy and radioprotection in space. Thanks to its tabletop setup, the FOOT experiment can be mounted at research cen-

\*e-mail: Riccardo.Ridolfi@bo.infn.it

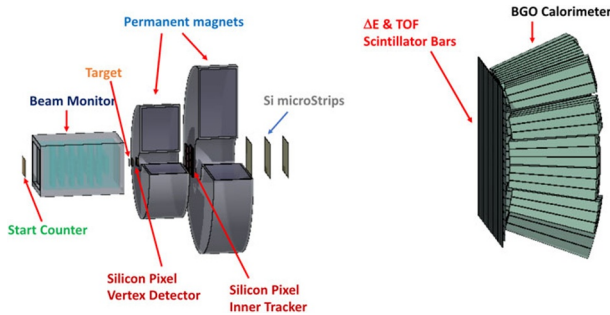


**Figure 1.** Schematic view of the FOOT electronic setup [1].

tres and at clinical facilities to harness the available variety of beams and energies. Indeed, the core program of the experiment foresees the use of  $^4\text{He}$ ,  $^{12}\text{C}$  and  $^{16}\text{O}$  beams with C,  $\text{C}_2\text{H}_4$  and PMMA targets to measure fragmentation cross sections in different energy ranges both for hadrontherapy (200 – 400 MeV/u) and for space radioprotection (700 – 800 MeV/u). Thanks to its flexibility, the experiment will be able to extend its physics program to other beam-target settings to possibly cover other data gaps.

FOOT will be able to measure both target fragmentation in proton treatments by means of an inverse kinematic approach and projectile fragmentation in hadrontherapy from direct kinematics approach. Moreover, measurements performed with FOOT will be also interesting for radioprotection in space, especially for light fragments produced by ions up to Oxygen. To achieve its goal FOOT will measure differential cross sections with respect to the kinetic energy  $d\sigma/dE_{\text{kin}}$  for the target fragmentation process with an accuracy better than 10% and double differential cross sections  $d^2\sigma/d\Omega dE_{\text{kin}}$  for the projectile fragmentation process with an accuracy better than 5% on the determination of the fragment yields in angle and in kinetic energy.

## 2.1 The electronic setup

The electronic setup was designed to detect and identify fragments heavier than  $^4\text{He}$  with an angular acceptance up to a polar angle of  $10^\circ$ .

To fit the strict requirements of measurement precision and ease of movement, the FOOT setup includes a  $\Delta E$ -TOF system and a calorimeter to measure the velocity, the charge and the kinetic energy of the fragment together with a magnetic spectrometer equipped with three tracking stations and two permanent magnets to provide a measure of the momentum of the fragments. A schematic view of the electronic setup is shown in Fig. 1.

### 2.1.1 Start Counter and Beam Monitor

The Start Counter (SC), placed at the very beginning of the setup, provides the minimum bias trigger of the experiment and the start time for the Time Of Flight (TOF) measurement. The SC is made by a thin foil of EJ-228 plastic scintillator 250  $\mu\text{m}$  thick with an active surface of

$5 \times 5 \text{ cm}^2$ . The light produced in the scintillator is collected laterally by 48  $3 \times 3 \text{ mm}^2$  SiPMs. The readout and the power supply of the SiPMs is handled by the WaveDAQ system [2], which is able to sample signals at rates up to 5 GS/s in a dynamic range of 1 V.

The Beam Monitor (BM) is a drift chamber consisting of twelve wire layers able to reconstruct the beam direction in both views. The BM efficiency is higher than 90% for a wide range of beams and energies while a lower limit on the spatial resolution of 100  $\mu\text{m}$ , in the central part of the BM cell, has been achieved [3].

The BM detector will be placed between the SC and the target and will be used to measure the direction and interacting point of the beam ions on the target while rejecting beam fragmentation before the target. The BM high spatial resolution is of great importance to measure the direction of the fragments with respect to the beam with an accuracy of few mrad which is necessary to measure the kinetic energy of the fragments in inverse kinematic with the required resolution.

### 2.1.2 Vertex detector, Inner Tracker and magnetic system

The Vertex detector (VTX) is organized in 4 pixel sensor layers covering an area of  $2 \times 2 \text{ cm}^2$ , placed along the z axis, respectively at 0.6 – 0.9 – 2.1 – 2.4 cm from the target center ensuring a geometrical acceptance of about  $40^\circ$  for the produced fragments. The Inner Tracker (ITR) foresees two planes of the same pixel sensors to track the fragments between the two magnets at a distance of about 15 cm from the target covering a sensitive area of about  $8 \times 8 \text{ cm}^2$ . In order to fulfill the required performances and constraints, the technology of the MIMOSA-28 (M28) Monolithic Active Pixel Sensors (MAPS) has been chosen for these detectors [1]. The magnetic system of the experiment is composed by two permanent magnets in Halbach configuration providing respectively a maximum intensity of 1.4 T and 0.9 T along the y axis in the internal cylindrical hole.

### 2.1.3 Micro Strip Detector

After the magnets, a third tracking station is present: this is essential both to measure the momentum of fragments and to match them with the hits in the  $\Delta E$ -TOF detector and in the calorimeter. For such a tracking station a microstrip silicon detector (MSD), which can also provide a redundant measurement of  $dE/dx$  thanks to its analog readout, was chosen. The detector is composed by three x-y planes with an active area of  $9.6 \times 9.3 \text{ cm}^2$ , separated by a 2 cm gap along the beam direction and positioned right after the second magnet. In order to reduce the amount of material and to provide the x-y coordinate readout, a setup with two perpendicular 150  $\mu\text{m}$  thick Single-Sided Silicon Detector (SSSD) sensors has been adopted for each MSD x-y plane. A strip pitch size of 50  $\mu\text{m}$  has been chosen in order to minimize the fragment pile-up in the same strip. For each SSSD, one every three strips is read for a total of 640 channels.

### 2.1.4 ToF Wall

The ToF Wall detector (TW) is composed of two layers of 20 plastic scintillator bars (EJ-200 by Eljen Technology), arranged orthogonally and wrapped with reflective aluminum and darkening black tape. Each bar is 0.3 cm thick, 2 cm wide and 44 cm long. The two orthogonal x-y layers form a  $40 \times 40 \text{ cm}^2$  active area detector that provides the measurements of the energy deposited  $\Delta E$ , the stop time to compute the TOF (the start time is provided by the SC), and the hit position. The TW transverse dimensions have been chosen to match the angular aperture of the heavy fragments at the distance of the detector from the target (1–2 m) depending on experimental room conditions. The simultaneous measurement of  $\Delta E$  and TOF allows to identify the charge  $Z$  of the ions crossing the detectors. The TW performances meet the FOOT requirements of a TOF resolution better than 100 ps and an energy loss resolution  $\sigma(\Delta E)/\Delta E \approx 5\%$ , for the heavier fragments.

### 2.1.5 Calorimeter

The FOOT calorimeter is the most downstream detector and it is designed to measure the kinetic energy of the fragments, providing a necessary information to compute their mass  $A$ .  $\text{Bi}_4\text{Ge}_3\text{O}_{12}$  (BGO) was chosen as the best material: the FOOT calorimeter will be composed by 320 BGO crystals covering an almost circular area of  $\approx 20 \text{ cm}$  radius. The crystals have a truncated pyramid shape with a front (back) area of about  $2 \times 2 \text{ cm}^2$  ( $3 \times 3 \text{ cm}^2$ ) and a length of 24 cm, chosen to minimize the energy leakage mainly due to neutrons escaping the calorimeter. The calorimeter will be readout by the WaveDAQ system as the SC and TW detectors at a rate of 1 GS/s in order to sample the full waveform. Several beam tests with different ions and energies were performed showing a very good linearity response and a energy resolution  $\sigma(E_{\text{kin}})/E_{\text{kin}}$  below 2% for heavier fragments.

## 3 First analysis of GSI2021

In July 2021 the FOOT collaboration had the possibility to perform measurements on beam at GSI in Darmstadt using  $^{16}\text{O}$  beam. The data taking involved a reduced apparatus of the FOOT electronic setup. Indeed, since the magnets, the Inner Tracker (IT) and the full Calorimeter (CALO) will be available within 2023, the setup was composed by the Start Counter (SC), the Beam Monitor (BM), the Vertex Detector (VTX), the Micro Strip Detector (MSD), the ToF Wall (TW) and one module (9 crystals) of the CALO. A preliminary analysis using the SC, BM and TW on a subset of data (400 MeV/u  $^{16}\text{O} + \text{C}$ ) is presented in the following.

### 3.1 MC simulations

The main information to extract from FLUKA Monte Carlo (MC) simulations are detection efficiencies for cross section calculations. In this context the efficiency was measured as follows:

$$\varepsilon(Z) = \frac{N_{\text{TW}}(Z)}{N_{\text{track}}(Z)} \quad (1)$$

where  $N_{\text{TW}}(Z)$  are the fragments with charge  $Z$  correctly reconstructed by the TW produced by primary particle in the target and  $N_{\text{track}}(Z)$  are the fragments generated by MC emitted from the target within the TW solid angle.

To not depend on fragmentation models in MC for the efficiency evaluation, for all MC analysis only fragments produced in the target were considered excluding secondary fragmentation outside the target. To extract  $N_{\text{TW}}$ , the number of TW points satisfying the same conditions of  $N_{\text{track}}$  were counted for each  $Z$ . Moreover, to not depend on the charge identification algorithm efficiency (even though it results to be high)  $N_{\text{TW}}$  were considered taking the true charge. This means that reconstruction efficiency should account for acceptance (both angular and in kinetic energy), intrinsic detector efficiency and clustering algorithm reconstruction efficiency. The same efficiency is then calculated for every angle for each charge for the differential cross section in angle.

### 3.2 GSI data

In the GSI2021 data taking the FOOT collaboration collected more than 40 million events using Carbon (C) and Polyethylene ( $\text{C}_2\text{H}_4$ ) targets with  $^{16}\text{O}$  beam at 200 and 400 MeV/u.

For this analysis, only runs with 400 MeV/u Oxygen beams on a Carbon target were selected. The goal of the preliminary analysis is to evaluate both angular and integrated elemental cross sections since there were no detectors providing the momentum or the kinetic energy of produced fragments. To this end, the elemental cross section for each  $Z$  can be written as follows:

$$\Delta\sigma(Z) = \int_{\beta_{\min}}^{\beta_{\max}} \int_0^{\theta_{\max}} \left( \frac{\partial^2 \sigma}{\partial \theta \partial \beta} \right) d\theta d\beta = \frac{Y(Z)}{N_{\text{prim}} \cdot N_{\text{TG}} \cdot \varepsilon(Z)} \quad (2)$$

where  $\theta_{\max}$  is the maximum TW detector acceptance angle ( $4.85^\circ$ ),  $\beta_{\min}$  and  $\beta_{\max}$  are the minimum and maximum velocity, respectively, corresponding to the  $T_{\text{tof}}$  range in which charge identification algorithm works properly (0.3 – 0.9),  $Y(Z)$  is the number of fragments of a given charge measured by TW,  $N_{\text{prim}}$  is the number of primaries impinging on the target,  $\varepsilon(Z)$  is the total efficiency for a given charge as calculated in the previous section and  $N_{\text{TG}}$  is the number of interaction centres in the target per unit surface which can be written as

$$N_{\text{TG}} = \frac{\rho \cdot \Delta x \cdot N_A}{A} \quad (3)$$

where  $\rho = 1.83 \text{ g/cm}^3$  is the graphite target density,  $\Delta x = 0.5 \text{ cm}$  is the target thickness,  $N_A$  is the Avogadro number and  $A = 12.0107$  is the graphite mass number.

Regarding angular elemental differential cross section, in Eq. 2 only integration in velocity is performed leading to the following formula:

$$\frac{d\sigma}{d\theta}(Z) = \frac{Y(Z, \theta)}{N_{\text{prim}} \cdot N_{\text{TG}} \cdot \Delta\theta \cdot \varepsilon(Z, \theta)} \quad (4)$$

where  $Y(Z, \theta)$  is the number of fragments of a given charge measured by TW within a given angle,  $\varepsilon(Z, \theta)$  is the efficiency for a given charge in a given angle and  $\Delta\theta$  is the

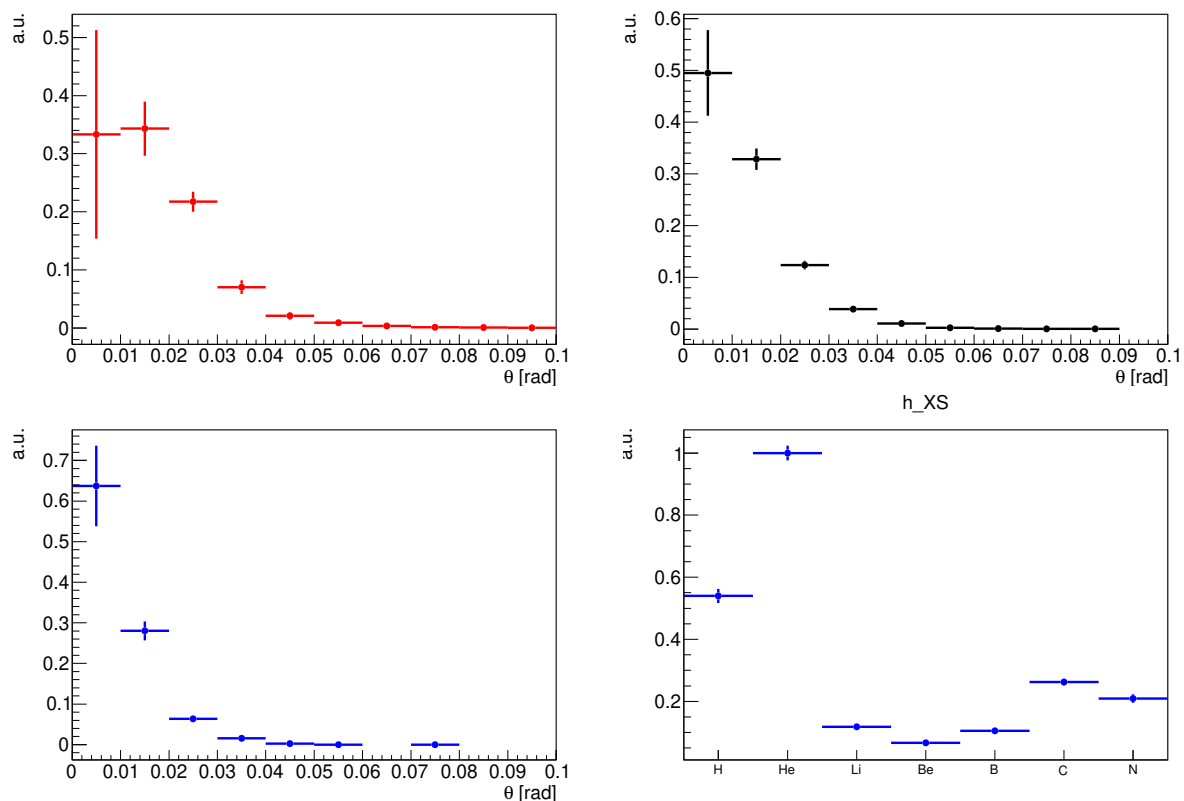


**Figure 2.** Preliminary angular differential cross sections for  $Z = 5$ ,  $Z = 6$ ,  $Z = 7$  and total integrated cross sections.

bin width. The bin width was set to 10 mrad ( $\approx 0.57^\circ$ ) since it represents the angle covered by a TW unit at the target-TW distance.

Since tracking detectors are not included in this analysis a strategy to remove the background composed by primary beam fragmentation outside the target had to be developed. Indeed, the out-of target fragmentation turns to be not negligible given the path length of fragments travelling in air and in detectors accounting for almost 30% of the total number of fragmentations. For this reason, a run without target was included in the analysis to subtract the background contribution. A preliminary result of differential cross sections accounting for statistical errors only is reported in Fig. 2. Since the systematic uncertainties are still being evaluated, angular differential cross sections are normalized to the unit area to highlight their shape while total integrated cross section is normalized to the highest value.

The preliminary results show that the FOOT setup is able to properly address cross section measurements which will be presented in a future work.

## 4 Acknowledgments

The FOOT Collaboration acknowledges the INFN for its support in building and running the detector, the Open Physics Hub (OPH) for the support and the GSI laboratory. The GSI data were taken in the IBER\_009 experiment, supported by European Space Agency (ESA)-IBER19 project, in the frame of FAIR Phase-0.

## References

- [1] G. Battistoni, M. Toppi, V. Patera, T.F. Collaboration, *Frontiers in Physics* **8**, 555 (2021)
- [2] L. Galli, A. Baldini, F. Cei, M. Chiappini, M. Francesconi, M. Grassi, U. Hartmann, M. Meucci, F. Morsani, D. Nicolò et al., *Nuclear Instruments and Methods in Physics Research Section A: Accelerators, Spectrometers, Detectors and Associated Equipment* **936**, 399 (2019)
- [3] Y. Dong, S. Gianluigi, C. Sofia, A. Andrey, A. Behcet, A. Giovanni, A. Stefano, R. Arteché Diaz, B. Mattia, B. Nazar et al., *Nuclear Instruments and Methods in Physics Research Section A: Accelerators, Spectrometers, Detectors and Associated Equipment* **986**, 164756 (2021)